Ferroelectric polarization reversal in multiferroic $MnWO_4$ via a rotating magnetic field up to 52 T

J. F. Wang,[1] W. X. Liu,[1] Z. Z. He,[2,*] C. B. Liu,[3] M. Tokunaga,[4] M. Li,[5] C. Dong,[1] X. T. Han,[1] F. Herlach,[1] C. L. Lu,[1] Z. W. Ouyang,[1] Z. C. Xia,[1] K. Kindo,[4] L. Li,[1] and M. Yang[1,†]

[1]*Wuhan National High Magnetic Field Center and School of Physics, Huazhong University of Science and Technology, Wuhan 430074, China*

[2]*State Key Laboratory of Structural Chemistry, Fujian Institute of Research on the Structure of Matter, Chinese Academy of Sciences, Fuzhou, Fujian 350002, China*

[3]*School of Physics and Electronic Engineering, Nanyang Normal University, Nanyang 473061, China*

[4]*The Institute for Solid State Physics (ISSP), University of Tokyo, Chiba 277-8581, Japan*

[5]*Department of Physics and Physical Oceanography, Memorial University, St. John's, Newfoundland, Canada A1B 3X7*

(Received 23 February 2021; accepted 1 July 2021; published 13 July 2021)

A long-standing issue in multiferroic $MnWO_4$ is the electric polarization reversal when magnetic field is applied along the magnetic easy axis ($H||u$). In this work, we performed comprehensive ferroelectric polarization measurements on $MnWO_4$ in fields up to 52 T and with rotating field direction in the *ac* plane. When the field is rotated from $H||c$ to $H||u$, the induced high-field phase ($-P||b$) favors a sign reversal relative to the low-field $+P||b$ phase, which is attributed to the vector spin chirality changing from one side of the spin connecting vector to the other. Particularly, further slight deviation of the field from the magnetic easy axis towards $H||a$ causes an abrupt reversal of the high-field phase from $-P||b$ to $+P||b$. We assume that this unusual angular dependence of polarization behavior can be understood by magnetic control of the helicity of the chiral plane with opposite conical spin structures. In addition, we also propose electric-field control of the chiral plane close to the ferroelectric phase transition at high fields. This study results in an overall understanding of this important multiferroic material and sheds light on field-induced polarization switching in related compounds.

DOI: 10.1103/PhysRevB.104.014415

I. INTRODUCTION

One of the most intriguing phenomena in multiferroic materials is the magnetic-field (H) induced electric polarization (P) switching, reorientation of P by 90° (flop) or 180° (reversal), that has been observed since the discovery of magnetoelectric coupling in the rare-earth manganites [1,2]. This magnetic control of ferroelectricity without changing the H direction has so far been observed in $RMnO_3$ (R = Tb, Dy) [1,3], RMn_2O_5 (R = Tb, Tm, Yb, Bi) [2,4–6], $MnWO_4$ [7,8], and other multiferroic materials [9–12]. Due to the complexity of the spin structures, however, theoretical explanations of these effects are a challenge [13–16]. Recently, the observation of the P switching in $Co_2V_2O_7$ was assumed to correlate with magnon Bose-Einstein condensation [17]; the concept of multiferroic quantum criticality was proposed and accounted for the high-field P reversal in $BiMn_2O_5$ [6,18]. To date, understanding the microscopic interplay between magnetism and electricity in these materials is essential and still an open issue.

The huebnerite $MnWO_4$ is a very rare multiferroic material that exhibits not only polarization flop but also reversal by application of a magnetic field. Specifically, this compound crystallizes into a monoclinic $P2/c$ space group with β between a and c being ~91° [19]. As shown in Fig. 1(a), the MnO_6 octahedra form zigzag chains along c with the nonmagnetic WO_6 located between the chains. At $H = 0$, $MnWO_4$ undergoes three transitions at 13.5, 12.7, and 7.6 K with magnetic ordering of the Mn^{2+} ($S = 5/2$) ions into incommensurate (AF3, AF2) and commensurate (AF1) phases [7,19]. The magnetic easy axis (*u axis*) lies in the *ac* plane and tilts at an angle of ~55° from the c axis, as illustrated in Fig. 1(b). In AF1 and AF3, the spins are antiferromagnetically aligned along the easy axis whereas in AF2 an elliptical spiral spin configuration towards the b axis is formed. Thus, AF2 is ferroelectric (FE) and spontaneous P is induced along b according to the Dzyaloshinskii-Moriya mechanism: $P \propto e_{ij} \times (S_i \times S_j)$, where e_{ij} is a vector that connects the spins S_i and S_j [20]. When H is applied along the b axis, polarization flop is observed by a change of the P direction from b to a at $H_f = \sim 11$T [7]. This corresponds to a FE phase transition from AF2 ($P||b$) to the so-called X phase ($P||$a) [21]. Another interesting discovery is the P reversal when H is applied along u (normal to the b axis) at 4.2 K. Apart from a nonpolarized HF phase, a FE phase of IV ($P||b$) was explored at $H = 38-48$ T and found to show opposite polarity to that of AF2 [8]. Although experimental and theoretical efforts have been made [22–25], the reason for this high-field polarization reversal remains unclear.

Rotation of the H direction yields more interesting information regarding $MnWO_4$. When H is rotated in the *ab* plane, a small deviation of H from the b axis (−2° to +2°) causes a P reversal of the flopped X phase [26]. Further, a continuous scan of H from a to $-a$ within the *ab* plane gives rise to a

*hezz@fjirsm.ac.cn
†ming_yang@hust.edu.cn

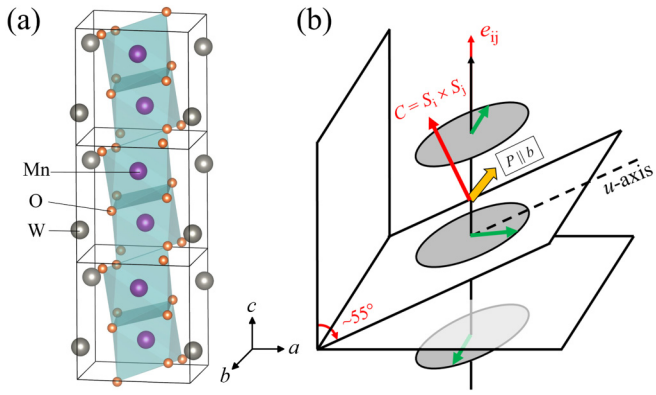

FIG. 1. (a) Crystal structure of $MnWO_4$ showing the zigzag chain along the c axis. The oxygen atoms surrounding each W^{6+} are not shown for clarity. (b) Schematic magnetic structure of the AF2 phase with a spontaneous electric polarization P (the orange arrow) along the b axis. The green arrows represent spins showing elliptical spiral structure in the ub plane while the u axis is the magnetic easy axis and canted to the c axis by ~55° [7]. Note that the spin connecting vector e_{ij} is parallel to c.

P reversal of AF2 for $H > H_f$ [27]. These results seem to closely combine the P flop and reversal via rotating the H direction in a peculiar crystallographic plane. Taniguchi *et al.* proposed two possible spiral spin structures for the X phase [26], where the P direction is determined by the vector spin chirality $C(= S_i \times S_j)$. Consequently, magnetic control of the C direction leads to the P reversal in slanted magnetic fields accompanied by a magnetoelectric memory [27].

In this contribution, we adopt a different strategy to rotate the H direction in the ac plane where large frustrations exist. Particularly, we extend magnetic fields up to 52 T to investigate a long-standing issue-the P reversal of phase IV. Our results elucidate how this reversal appears when H is rotated from c to u without considering the P flop and the memory effect. Remarkably, we uncover that, when H is further canted towards the a axis, phase IV suddenly changes its polarity, which is attributed to a change of the helicity of the spiral spin structure under a strong magnetic field.

II. EXPERIMENT

Single crystals of $MnWO_4$ in dark red were grown by a flux method and characterized by the x-ray single-crystal diffraction. The crystals are oriented and cut into thin plates with a dimension of $2\times1.5\times0.2$ mm^3. High-field electric polarization was measured by the pyroelectric technique using a 10.5-ms pulsed magnet at the Wuhan National High Magnetic Field Center (WHMFC), China. In the experiments, the sample was first cooled down under a finite electric field (E). As the sample reaches the ferroelectric AF2 phase, this electric field was removed before the pulse shot and the variation of P with H was measured. While as the sample is in the paraelectric AF1 phase, the electric field was maintained during the pulse in order to fully polarize the FE domains induced by a magnetic field. When P occurs in a pulsed field charges will flow in the circuit and a pyroelectric current was detected by a 10-kΩ shunt resistor, which was then integrated to obtain the P (H) curve. This experimental technique has been successfully developed in the WHMFC and more details may be found elsewhere [28]. A high precision quartz rotator was used in our experiments for the angular dependent measurements of P (H).

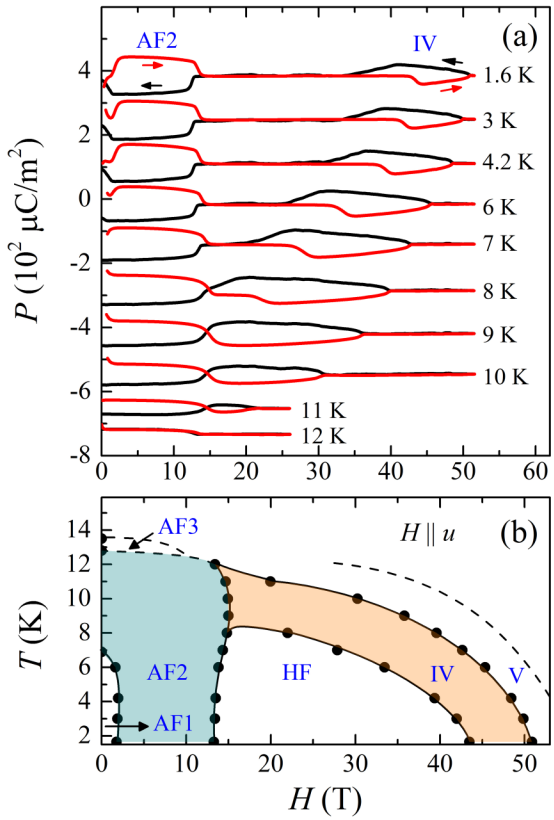

FIG. 2. (a) The P (H) curves measured in various temperatures. Magnetic field is applied along the magnetic easy axis ($H||u$). A bias electric field of $E = +500$ kV/m is applied and maintained during each pulse shot. The red (black) curve denotes the increasing (decreasing) fields. Data are offset vertically. (b) The H-T phase diagram constructed from the rising field sweeps. The FE phases (AF2 and IV) are marked in colors. The dashed boundaries for phases AF3 and V are taken from Ref. [23].

III. RESULTS

A. Magnetic phase diagram at $H||u$

We first measured the electric polarization ($P||b$) of $MnWO_4$ in magnetic fields applied along the magnetic easy axis ($H||u$). Figure 2(a) shows the P (H) curves measured at various temperatures. At 1.6 K, two magnetic field-induced FE phases are clearly observed as indicated by AF2 and IV. In a rising sweep (the red curve), AF2 (2−13 T) and IV (43−51 T) have opposite polarities whereas in a falling sweep (the black curve) AF2 and IV both reverse the P direction, signifying a "∞"-type loop in one field cycle. In a test experiment at 4.2 K, we find that the P directions of AF2 and IV are always reversed independent with the peak magnetic fields or applied electric fields. As temperature is increased, AF2 and IV connect to each other at 8 K and finally converge at 12 K.

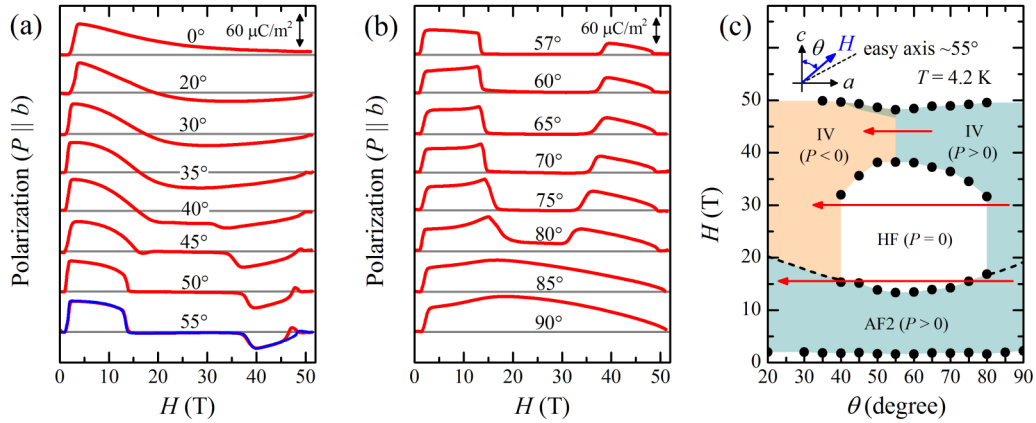

FIG. 3. (a), (b) The H dependence of P in the rising sweep at 4.2 K by rotating H in the ac plane ($E = +1\text{MV/m}$). θ is the angle between H and the c direction. Data are vertically offset with the grey lines at $P = 0$. The red curve for 55° is a subsequent measurement with $E = 0$. (c) The H-θ phase diagram at 4.2 K. The solid dots are derived from the magnetic transitions in (a) and (b) while the dashed lines show the phase boundaries. The colors show the polarity of P. The polarity of the small grey area at ~50 T is sensitive to E. The red arrows represent several paths with rotating H direction.

Note that even at a temperature up to 11 K AF2 and IV exhibit opposite polarities for either the rising or the falling sweep.

Derived from Fig. 2(a), we construct the H-T phase diagram of $MnWO_4$ for $H||u$ and show the result in Fig. 2(b). Besides AF2 and IV, the nonpolarized AF1 and HF phases are obtained. Another two paraelectric ordered phases (AF3 and V), which were determined previously [23], are also shown for a comparison. It is found that our experimental data for $H||u$ and the corresponding phase diagram are basically in agreement with those reported in previous papers [8,23,29].

B. Magnetic angular rotation in the *ac* plane at 4.2 K

The most striking observation in our experiments is that as the magnetic field direction is a little more canted from the magnetic easy axis in the ac plane the P reversal of phase IV suddenly disappears. Instead, the polarizations of AF2 and IV are both positive for either increasing or decreasing fields which is completely different from the behavior for $H||u$. This unusual angular dependence of the P switching motivates us to perform a systematic measurement by rotating the H direction from c to a.

Figure 3(a) shows the P (H) curves of $MnWO_4$ by rotating H from c ($\theta = 0°$) to u ($\theta = 55°$), where θ is defined as the angle between c and H. For $\theta = 0°$, H induces a FE phase transition at ~2 T and then P is reduced to almost zero up to 52 T. For $\theta = 20-40°$, a negative P begins to appear above 15−20 T. In a higher field, it undergoes a transition to a paraelectric state at ~50 T. From $\theta = 40°$, a plateau emerges between the positive and the negative P, which becomes large and maintains at $P = 0$ for $\theta = 45-55°$. Consequently, the evolution of P with the H angles ($0 - 55°$) well presents the formation of the four magnetic ordered phases (AF2, HF, IV, and V) as shown in Fig. 2(b), in particular the P reversal between AF2 and IV. Figure 3(b) shows the data for rotating H from 57° to 90° (nearly the a axis). It is noteworthy that the P reversal as shown in Fig. 3(a) is no longer observed for angles $\theta \geqslant 57°$. By contrast, the P direction of IV remains positive like that of AF2. As θ is increased, the two FE phases are somehow enhanced for the field range and the P amplitude. For $\theta \geqslant 85°$, the HF phase disappears while AF2 and IV converge.

Our experimental results evidently reveal two different scenarios due to rotating H in the ac plane. One is for $\theta \leqslant 55°$ that P favors a sign reversal in applied fields, while the other is that P preserves its direction for $\theta > 55°$. For a better view of this angular dependent relation, we summarize the H-θ phase diagram at 4.2 K in Fig. 3(c). We find that this H-θ phase diagram is helpful to understand the early experimental results as shown in later discussion.

C. Magnetic angular rotation in the *ac* plane at 8.8 K

In order to verify the above angular dependence, we further measured the polarization behavior of $MnWO_4$ at 8.8 K. At this temperature, a spontaneous P exists at $H = 0$ and no HF phase will be induced by magnetic fields as seen in Figs. 2(a) and 2(b). Figure 4(a) shows the P (H) data for several

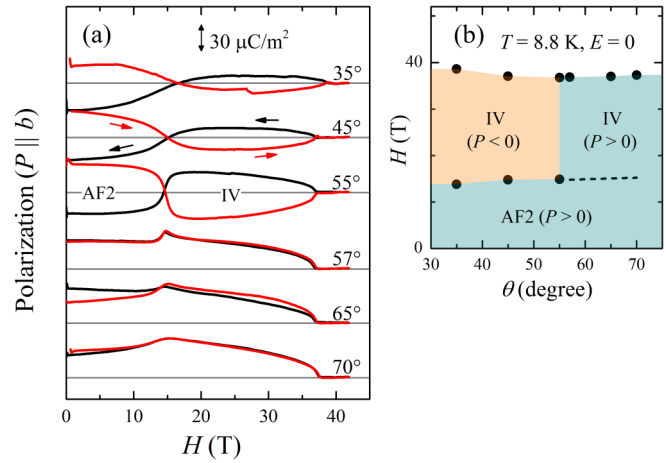

FIG. 4. (a) P (H) measured at 8.8 K for selected H directions. (b) The H-θ phase diagram at 8.8 K derived from the data for increasing fields. The dashed line shows the peak anomaly in the P (H) curve.

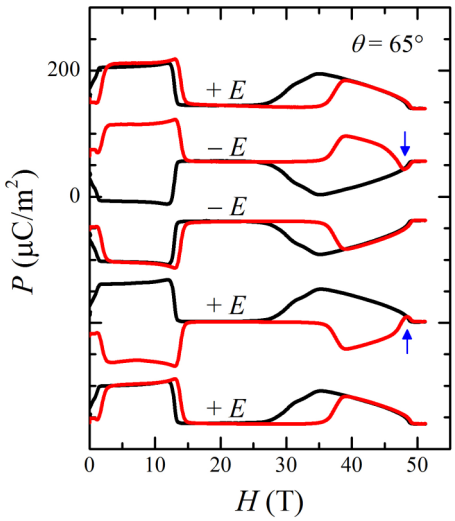

FIG. 5. Electric-field control of the P reversal in five successive pulses (from up to bottom, $|E| = 1\text{MV/m}$). The arrow shows the anomaly at the FE transition to the nonpolarized state. The red (black) curve is for increasing (decreasing) fields. Data are vertically offset.

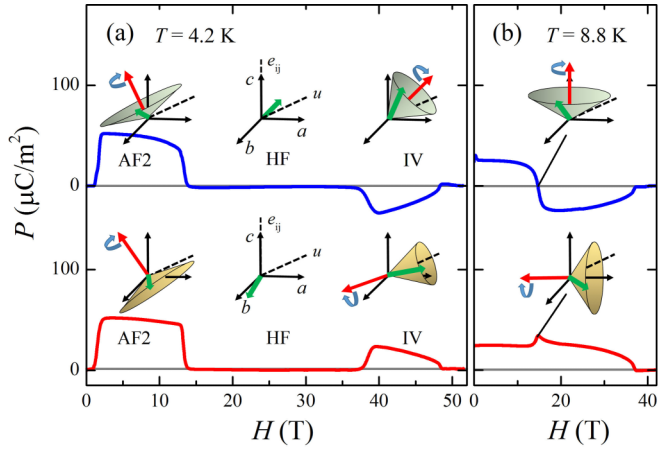

FIG. 6. Schematic evolutions of proposed field-induced spin structures for $\theta = 55°$ (upper) and 57° (bottom). (a), (b) denote 4.2 and 8.8 K. The conical spin structures are responsible for the AF2 and IV phases, where the green and the red arrows represent the spin and the vector spin chirality ($C = S_i \times S_j$).

H rotation angles. For $\theta \leqslant 55°$, it is found that the polarities of AF2 and IV are opposite, indicative of a reversal of P. In addition, the H-decreasing curve is also opposite to the H-increasing curve, showing a "∞"-type loop. For $\theta \geqslant 57°$, however, this relation between AF2 and IV is suddenly removed. Interestingly, AF2 and IV both show a positive polarization with a maximum value at ∼15 T which corresponds to a phase transition from AF2 to IV. Furthermore, the "∞"-type loop disappears and the H-increasing and -decreasing curves almost overlap (see the data for 57° and 70°). We assume that a relative big noise occurs in the decreasing field and results in a small deviation of the data for $\theta = 65°$. These distinct polarization behaviors between $\theta \leqslant 55°$ and $\theta > 55°$ at 8.8 K are consistent with those experimental observations at 4.2 K [see Figs. 3(a) and 3(b)], demonstrating a unique magnetic angular dependence associated with the magnetic easy axis (u axis) in $MnWO_4$.

The derived H-θ phase diagram at 8.8 K is presented in Fig. 4(b). Due to lack of the HF phase, the phase boundary of AF2 to IV is nearly angular independent and the resultant diagram looks simple in comparison with the result of 4.2 K in Fig. 3(c).

D. Polarization reversal by an electric field

As shown in Fig. 3(a), an anomaly with a small component of $+P$ is visible at ∼50 T upon application of $E = +1\text{MV/m}$ for $\theta = 45°$–$55°$. For $\theta = 55°$, we performed a subsequent measurement with $E = 0$ (the blue curve). Except for the anomaly, P (H) is fully recovered owing to a memory effect. Nevertheless, this kind of anomaly is not observed at ∼50 T for $\theta > 55°$ as shown in Fig. 3(b). Following the work in Ref. [28], we performed electric-field control of the polarization reversal in $MnWO_4$ at 4.2 K by successive five pulse shots. Figure 5 displays the P reversal under the influence of E measured for $\theta = 65°$. For the first pulse, P (H) in a falling sweep almost follows the trace of the rising sweep except a hysteresis seen at the first-order transition. When E is reversed to $-E$, P (H) in the rising sweep is almost retained due to the memory effect. However, at the IV-V phase transition (see the arrow) an anomaly with a $-P$ component appears, similar to the observation for $\theta = 55°$. Since the IV-V transition is of the second order, we do not need to consider the existence of ferroelectric embryos above 50 T. Thus the polarization polarity in the falling sweep can be switched by applied electric field. Under the next $-E$, P (H) in the rising sweep is also reversed. The above process is repeatable when we continue to reverse the electric field from $-E$ to $+E$. Indeed, a small $+P$ component again appears at the IV-V transition which leads to a P reversal in the falling sweep. For the fifth pulsed field under $+E$, P (H) is recovered to the initiate state. These experimental results, reminiscent of a two-step polarization reversal in $Ni_3V_2O_8$ [28], demonstrate that the polarization polarity close to the IV-V phase transition (second order) can be switched by an electric field.

IV. DISCUSSION

Mitamura *et al.* proposed a phenomenological model to explain the sign reversal of phase IV for $H||u$ [23]. As illustrated in Fig. 6 (the blue curve), in AF2 spins initially rotate elliptically (clockwise) in the ub plane and then form a conical spin arrangement in magnetic fields. Considering $P \propto e_{ij} \times C (e_{ij} = c \text{ axis})$, a positive P along b will occur. A strong magnetic field may change C from the left side of e_{ij} to the right, leading to a reversal of P in phase IV. At 8.8 K [Fig. 6(b)], C varies continuously and a $P = 0$ state is expected for $C||e_{ij}$. At 4.2 K [Fig. 6(a)], the nonpolarized HF phase emerges which has spins approximately oriented along b as demonstrated theoretically and experimentally (the spins are further aligned towards the H direction in a high magnetic field) [24,30]. Our angular data in Fig. 3(a) support this model perfectly. Indeed, rotating H from u to c suppresses the negative P; for $H||c$, no reversal is observed because C cannot

move to the right side of e_{ij}. To understand the results for $\theta > 55°$, we consider a different situation as depicted in Fig. 6 (the red curve). In this H direction, the conical spin structure of AF2 is naturally opposite to that for $\theta \leqslant 55°$ under the field alignment. Due to the fact that C is gradually modulated by H, it is essential that the helicity of the conical structure should be transformed to anticlockwise when H is rotated across the u axis. In the low-field region, the AF2 phase still shows a positive value in agreement with the experimental observation. However, in this case C gradually deviates away from e_{ij} as H is further increased, in contrast to the movement of C for the case of $\theta \leqslant 55°$. It is noted that even in a strong magnetic field C is located on the left side of e_{ij}. Recalling the relation $P \propto e_{ij} \times C$, this explains why the polarity of phase IV remains positive; the maximum of P at 8.8 K is due to the fact that C is perpendicular to e_{ij} exactly [Fig. 6(b)]. Another interesting observation is that the dP/dH of AF2 also depends on the H direction: $dP/dH < 0$ for $\theta < 55°$ and $dP/dH > 0$ for $\theta > 57°$. Similar dP/dH behavior was observed by Taniguchi *et al.* for H applied along the a and c axes [31]. We attribute these to the change of relative angle between C and e_{ij}, again supporting the proposed spin models in Fig. 6. Note that the small negative dP/dH for 57° is likely a combination result of the movement of C and close of the conical umbrella structure in applied magnetic fields.

Here we discuss the H-θ phase diagram and consider three measurement paths as the displayed red arrows in Fig. 3(c). For $H = 15$ T, a rotation of H ($H||\mathrm{a} \rightarrow H||u \rightarrow H||c$) will result in P (θ) to be $+P \rightarrow 0 \rightarrow +P$. As H is increased to 30 T, P (θ) then changes to be $+P \rightarrow 0 \rightarrow -P$. This P reversal in a dependence of θ resembles the previous study by Taniguchi *et al.* [27]: when H is rotated in the ab plane ($H||\mathrm{a} \rightarrow H||b \rightarrow H||-\mathrm{a}$), P is reversed above $H_f \sim 11$ T accompanied by a magnetoelectric memory effect. In a separate work, it is observed that when H is a little tilted across the b axis in the ab plane the H-induced X phase ($P||\mathrm{a}$) suddenly changes its polarity [26]. This phenomenon is similar to the P reversal of phase IV at around $H||u$, as shown in the third path for $H = 45$T. On the other hand, it was assumed by Mitamura *et al.* that phase X ($H||b$) and phase IV ($H||u$) may arise from the same origin and can be transformed to each other by rotating H in the ub plane [23]. Based on these results, we argue that the two methods of H rotation in the ac and ab planes are actually equivalent in controlling the vector spin chirality C of $MnWO_4$. Nevertheless, early study of the spin-wave excitations infers that magnetic frustration along either the c or a axis is actually much stronger than that between chains along the b axis [32]. A perturbation by external fields may destroy the balance of magnetic interactions and therefore yield an unexpected magnetoelectric response. In this respect, rotating H in the ac plane in present study employs a simple approach for the P reversal since it does not involve the P flop and the complex memory effect in the process. These results are also valuable to understand the mechanism of the P reversal in $TbMnO_3$ with rotating H in the ab plane ($H||b \rightarrow H||\mathrm{a} \rightarrow H||-b$) [33,34].

Our experiments also provide insight into the early theoretical calculation on $MnWO_4$ by Quirion *et al.* [24]. Using a nonlocal Landau free energy approach, they reproduced the high-field phase diagrams of $MnWO_4$ which are in good agreement with the experimental observations. This model includes a simplified low-order magnetoelectric coupling term F_{ME} with the free energy F_E expressed as

$$F_E = \frac{1}{2}\frac{P_a^2}{\chi_a} + \frac{1}{2}\frac{P_b^2}{\chi_b} + \frac{1}{2}\frac{P_c^2}{\chi_c} + F_{ME},$$

where $a - c$ represent the principal axes and χ is the susceptibility. Figure 7(a) presents the numerical calculations of P (H) at $T = 0$ and $T = 0.6$ for $\theta = 55°$ ($H||u$). The fact that the result is inconsistent with the experimental observations of a sign reversal of P suggests the existence of a high-order magnetoelectric coupling term $\zeta PP_{ME}m^2$ (sixth order) for $\theta = 55°$ [24]. However, this theoretical result is surprisingly in excellent agreement with our data for $\theta = 57°$ as shown in Fig. 7(b). This implies that the high-order term $\zeta PP_{ME}m^2$ should be missing when H is rotated to $\theta > 55°$. This probably reflects why the "∞"-type loop in P (H) suddenly disappears for $\theta > 55°$ while it always appears for $\theta \leqslant 55°$ even in absence of an electric field (see Fig. 4). Although, as shown in Ref. [24], the fourth-order Landau model without considering the magnetization (m) and the electric polarization (P) coupling is sufficient to reproduce the phase diagrams, these results indicate that due to the large value of the magnetization in a high-field region the contribution of $\zeta PP_{ME}m^2$ or higher order terms are important to describe the polarization behaviors of $MnWO_4$ at high fields. Detailed theoretical investigation based on these experimental data is highly desirable to clarify this point. Further, the Landau theory predicts a switch of the chiral plane from the ub plane in AF2 to a perpendicular plane in IV, which qualitatively agrees with the proposed spin models in Fig. 6.

We finally discuss the electric-field control of the polarization reversal in $MnWO_4$. This effect has a direct influence on the IV-V transition for a rising sweep, i.e., the anomalies

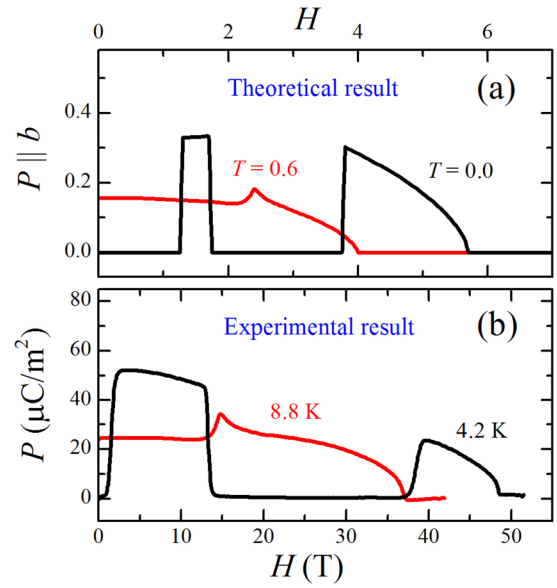

FIG. 7. A comparison of the previous theoretical result (a) and our experimental data (b). The curves in (a) are for $\theta = 55°$ and reproduced from Ref. [24] while those in (b) are for $\theta = 57°$.

at ∼50 T. Though it remains tiny, we point out that this anomaly plays a crucial role in the process of a falling sweep leading to a dramatic change of the polarity in zero electric field. As reported from a neutron diffraction experiment, an electric field may control the spin chirality of $MnWO_4$ near the AF2-AF3 phase transition [35,36]. With a view to the fact that spins are nearly field aligned at ∼50 T, it is likely that an electric field changes the helicity of the conical spin structure in phase IV. We believe that in $Co_2V_2O_7$ a similar anomaly at the FE phase transition and the loop in P (H) originate for the same reason [17].

V. CONCLUSION

In summary, we have measured electric polarization of $MnWO_4$ in magnetic fields up to 52 T and identified distinct polarization behaviors of the high-field ferroelectric phases with a rotating magnetic field in the *ac* plane: it shows a sign reversal for $\theta \leqslant 55^\circ$ but sustains the polarity for $\theta > 55^\circ$. These different scenarios are attributed to a direct modulation of the spin chiral plane (the *ub* plane) with opposite spin helicities. This was further demonstrated by an electric-field control of the chiral plane close to the high-field ferroelectric phase transition. These experimental findings improve understanding of the early experimental and theoretical results.

ACKNOWLEDGMENTS

J.F.W. would like to thank Z. Wang in the High Magnetic Field Laboratory of China (Hefei) for helpful discussions. This work was supported by the National Natural Science Foundation of China (Grants No. 12074135, No. U1832214, No. 21875249, No. 12004122, No. 51821005, and No. 11774106) and the Fundamental Research Funds for the Central Universities (Grants No. 2018KFYXKJC005 and No. 2019KFYXJJS009).

[1] T. Kimura, T. Goto, H. Shintani, K. Ishizaka, T. Arima, and Y. Tokura, Nature (London) **426**, 55 (2003).
[2] N. Hur, S. Park, P. A. Sharma, J. S. Ahn, S. Guha, and S.-W. Cheong, Nature (London) **429**, 392 (2004).
[3] F. Kagawa, M. Mochizuki, Y. Onose, H. Murakawa, Y. Kaneko, N. Furukawa, and Y. Tokura, Phys. Rev. Lett. **102**, 057604 (2009).
[4] M. Fukunaga, Y. Sakamoto, H. Kimura, Y. Noda, N. Abe, K. Taniguchi, T. Arima, S. Wakimoto, M. Takeda, K. Kakurai, and K. Kohn, Phys. Rev. Lett. **103**, 077204 (2009).
[5] M. Fukunaga, Y. Sakamoto, H. Kimura, and Y. Noda, J. Phys. Soc. Jpn. **80**, 014705 (2011).
[6] J. W. Kim, S. Y. Haam, Y. S. Oh, S. Park, S.-W. Cheong, P. A. Sharma, M. Jaime, N. Harrison, J. H. Han, G.-S. Jeon, P. Coleman, and K. H. Kim, Proc. Natl. Acad. Sci. USA **106**, 15573 (2009).
[7] K. Taniguchi, N. Abe, T. Takenobu, Y. Iwasa, and T. Arima, Phys. Rev. Lett. **97**, 097203 (2006).
[8] H. Mitamura, H. Nakamura, T. Kimura, T. Sakakibara, and K. Kindo, J. Phys.: Conf. Ser. **150**, 042126 (2009).
[9] S. Park, Y. J. Choi, C. L. Zhang, and S.-W. Cheong, Phys. Rev. Lett. **98**, 057601 (2007).
[10] Y. J. Choi, J. Okamoto, D. J. Huang, K. S. Chao, H. J. Lin, C. T. Chen, M. van Veenendaal, T. A. Kaplan, and S.-W. Cheong, Phys. Rev. Lett. **102**, 067601 (2009).
[11] K. Kimura, H. Nakamura, S. Kimura, M. Hagiwara, and T. Kimura, Phys. Rev. Lett. **103**, 107201 (2009).
[12] M. Kinoshita, S. Seki, T. J. Sato, Y. Nambu, T. Hong, M. Matsuda, H. B. Cao, S. Ishiwata, and Y. Tokura, Phys. Rev. Lett. **117**, 047201 (2016).
[13] M. Mochizuki and N. Furukawa, Phys. Rev. Lett. **105**, 187601 (2010).
[14] I. E. Chupis and H. A. Kovtun, Appl. Phys. Lett. **103**, 182901 (2013).
[15] J. H. Lee and H. M. Jang, Phys. Rev. B **91**, 014403 (2015).
[16] O. I. Utesov and A. V. Syromyatnikov, Phys. Rev. B **100**, 054439 (2019).
[17] R. Chen, J. F. Wang, Z. W. Ouyang, M. Tokunaga, A. Y. Luo, L. Lin, J. M. Liu, Y. Xiao, A. Miyake, Y. Kohama, C. L. Lu, M. Yang, Z. C. Xia, K. Kindo, and L. Li, Phys. Rev. B **100**, 140403(R) (2019).
[18] A. Narayan, A. Cano, A. V. Balatsky, and N. A. Spaldin, Nat. Mater. **18**, 223 (2019).
[19] G. Lautenschlger, H. Weitzel, T. Vogt, R. Hock, A. Böhm, M. Bonnet, and H. Fuess, Phys. Rev. B **48**, 6087 (1993).
[20] H. Katsura, N. Nagaosa, and A. V. Balatsky, Phys. Rev. Lett. **95**, 057205 (2005).
[21] I. Urcelay-Olabarria, E. Ressouche, A. A. Mukhin, V. Y. Ivanov, A. M. Kadomtseva, Yu. F. Popov, G. P. Voro'ev, A. M. Balbashov, J. L. Garcia-Munoz, and V. Skumryev, Phys. Rev. B **90**, 024408 (2014).
[22] H. Nojiri, S. Yoshii, M. Yasui, K. Okada, M. Matsuda, J.-S. Jung, T. Kimura, L. Santodonato, G. E. Granroth, K. A. Ross, J. P. Carlo, and B. D. Gaulin, Phys. Rev. Lett. **106**, 237202 (2011).
[23] H. Mitamura, T. Sakakibara, H. Nakamura, T. Kimura, and K. Kindo, J. Phys. Soc. Jpn. **81**, 054705 (2012).
[24] G. Quirion and M. L. Plumer, Phys. Rev. B **87**, 174428 (2013).
[25] N. V. Ter-Oganessian and V. P. Sakhnenko, J. Phys.: Condens. Matter **26**, 036003 (2014).
[26] K. Taniguchi, N. Abe, H. Umetsu, H. Aruga Katori, and T. Arima, Phys. Rev. Lett. **101**, 207205 (2008).
[27] K. Taniguchi, N. Abe, S. Ohtani, and T. Arima, Phys. Rev. Lett. **102**, 147201 (2009).
[28] Y. J. Liu, J. F. Wang, Z. Z. He, C. L. Lu, Z. C. Xia, Z. W. Ouyang, C. B. Liu, R. Chen, A. Matsuo, Y. Kohama, K. Kindo, and M. Tokunaga, Phys. Rev. B **97**, 174429 (2018).
[29] V. Felea, P. Lemmens, S. Yasin, S. Zherlitsyn, K. Y. Choi, C. T. Lin, and C. Payen, J. Phys.: Condens. Matter **23**, 216001 (2011).
[30] S. Toyoda, N. Abe, T. Arima, and S. Kimura, Phys. Rev. B **91**, 054417 (2015).
[31] K. Taniguchi, N. Abe, H. Sagayama, S. Ohtani, T. Takenobu, Y. Iwasa, and T. Arima, Phys. Rev. B **77**, 064408 (2008).

[32] F. Ye, R. S. Fishman, J. A. Fernandez-Baca, A. A. Podlesnyak, G. Ehlers, H. A. Mook, Y. Q. Wang, B. Lorenz, and C. W. Chu, Phys. Rev. B **83**, 140401(R) (2011).

[33] N. Abe, K. Taniguchi, S. Ohtani, T. Takenobu, Y. Iwasa, and T. Arima, Phys. Rev. Lett. **99**, 227206 (2007).

[34] N. Abe, K. Taniguchi, S. Ohtani, H. Umetsu, and T. Arima, Phys. Rev. B **80**, 020402(R) (2009).

[35] T. Finger, D. Senff, K. Schmalzl, W. Schmidt, L. P. Regnault, P. Becker, L. Bohatỳ, and M. Braden, Phys. Rev. B **81**, 054430 (2010).

[36] J. Stein, M. Baum, S. Holbein, T. Finger, T. Cronert, C. Tölzer, T. Fröhlich, S. Biesenkamp, K. Schmalzl, P. Steffens, C. H. Lee, and M. Braden, Phys. Rev. Lett. **119**, 177201 (2017).